Dynamical properties of neuron models–nodal and collective behaviours.

Indranil Ghosh

School of Mathematical and Computational Sciences
Massey University, Palmerston North, New Zealand

August 14, 2024

Neurons as Dynamical units

- Neurons represent the fundamental dynamical units of the nervous system
- The dynamics of neurons, like firing of action potentials, can be modeled as simple dynamical systems like ODEs or maps

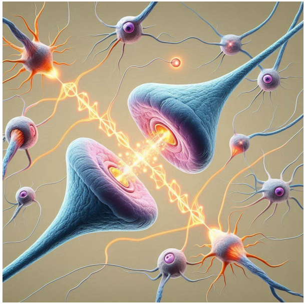

Figure: Two neurons connected by a synapse. (Powered by DALL-E 3)

Chialvo Map (Chialvo, 1995)

The two-dimensional neuron map is given by

$$\begin{aligned} x_{n+1} &= x_n^2 e^{(y_n - x_n)} + k_0, \\ y_{n+1} &= a y_n - b x_n + c. \end{aligned}$$

- The state variables x and y represent the activation variable and recovery-like variable,
- a, b, c and k_0 are the system parameters,
- $a < 1$ is the time constant of recovery,
- $b < 1$ represents the activation dependence of the recovery process,
- c denotes the offset, and
- k_0 is the time-independent additive perturbation.

A Typical Phase Portrait

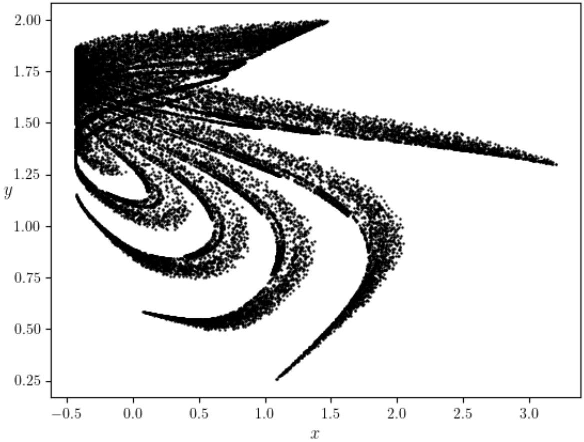

Electromagnetic flux

We describe the effects of electromagnetic flux on the system of neurons with **memristors**. The induction current due to electromagnetic flux is given by

$$\frac{dq(\phi)}{dt} = \frac{dq(\phi)}{d\phi}\frac{d\phi}{dt} = M(\phi)\frac{d\phi}{dt} = kM(\phi)x.$$

- ϕ: electromagnetic flux across the neuron membranes,
- k: electromagnetic flux coupling strength, &
- $M(\phi)$: memconductance of electromagnetic flux controlled memristor.

We consider the following memconductance function:

$$M(\phi) = \alpha + 3\beta\phi^2.$$

Improved Chialvo map under electromagnetic flux (Muni, Fatoyinbo, & Ghosh, 2022)

International Journal of Bifurcation and Chaos, Vol. 32, No. 9 (2022) 2230020 (26 pages)

DOI: 10.1142/S0218127422300208

Dynamical Effects of Electromagnetic Flux on Chialvo Neuron Map: Nodal and Network Behaviors

Sishu Shankar Muni[*,†,‡], Hammed Olawale Fatoyinbo[†,§]
and Indranil Ghosh[†,¶]
[*]*Department of Physical Sciences,*
Indian Institute of Science and Educational Research Kolkata,
Campus Road, Mohanpur, West Bengal 741246, India
[†]*School of Mathematical and Computational Sciences,*
Massey University, Colombo Road,
Palmerston North, 4410, New Zealand
[‡]*sishu1729@iiserkol.ac.in*
[‡]*s.muni@massey.ac.nz*
[§]*h.fatoyinbo@massey.ac.nz*
[¶]*i.ghosh@massey.ac.nz*

Received January 11, 2022 ; Revised May 4, 2022

Improved Chialvo map under electromagnetic flux (Muni, Fatoyinbo, & Ghosh, 2022)

Under the action of electromagnetic flux, the system of Chialvo map is improved to the following map:

$$
\begin{aligned}
x_{n+1} &= x_n^2 e^{(y_n - x_n)} + k_0 + k x_n M(\phi_n), \\
y_{n+1} &= a y_n - b x_n + c, \\
\phi_{n+1} &= k_1 x_n - k_2 \phi_n,
\end{aligned}
$$

making the system a three-dimensional smooth map. The new variables α, β, k_1, k_2 represent the electromagnetic flux parameters.

Multistability

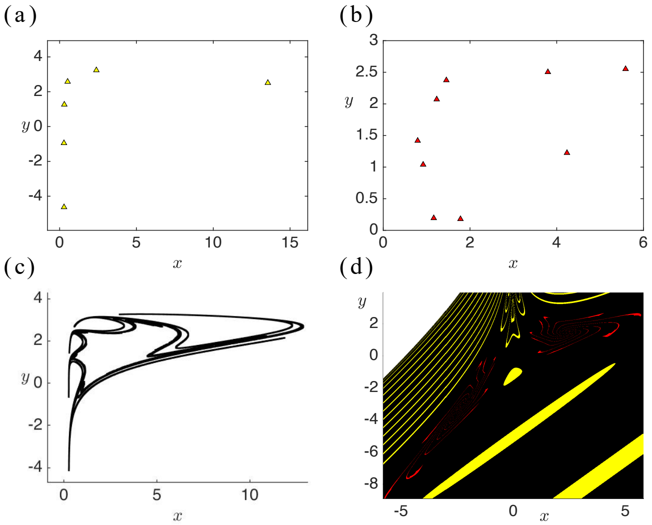

Bifurcation structures and antimonotonicity

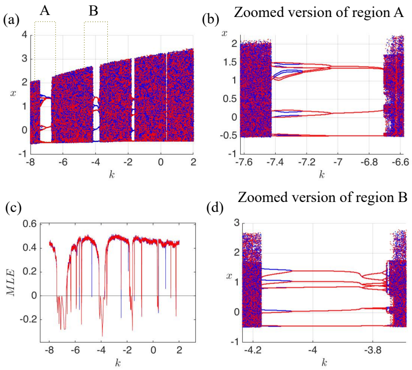

Figure: Bifurcation diagram of x with respect to k in panel (a). A maximal Lyapunov exponent diagram is shown in panel (b).

Bifurcation structures and antimonotonicity

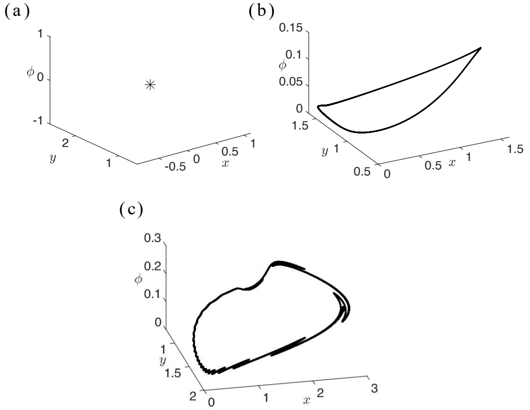

Figure: In (a) a stable fixed point is shown in the $x - y - \phi$ phase space for $a = 0.838$. After a supercritical Neimark-Sacker bifurcation, an attracting closed invariant curve is born as shown in (b) at $a = 0.841$. A chaotic attractor is then formed when a is increased to 0.88.

Numerical bifurcation analysis

Table: Abbreviations of codimension-1 and codimension-2 bifurcations

Codimension-1			
Saddle-node (fold) bifurcation	LP	Neimerk-Sacker bifurcation	NS
Period-doubling (flip) bifurcation	PD		
Codimension-2			
Cusp	CP	Chenciner	CH
Generalized flip	GPD	Fold-Flip	LPPD
Flip-Neimark-Sacker	PDNS	Fold-Neimark-Sacker	LPNS
1:1 resonance	R1	1:2 resonance	R2
1:3 resonance	R3	1:4 resonance	R4

Numerical bifurcation analysis

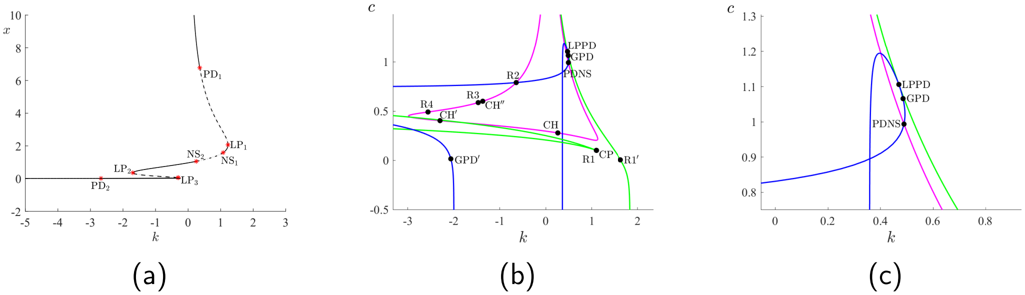

Figure: (a) Codimension-1 bifurcation diagram with k as bifurcation parameter. (b) Codimesion-2 bifurcation diagram in (k, c)-parameter plane. (c) Zoomed version of (b)

Bursting and spiking features

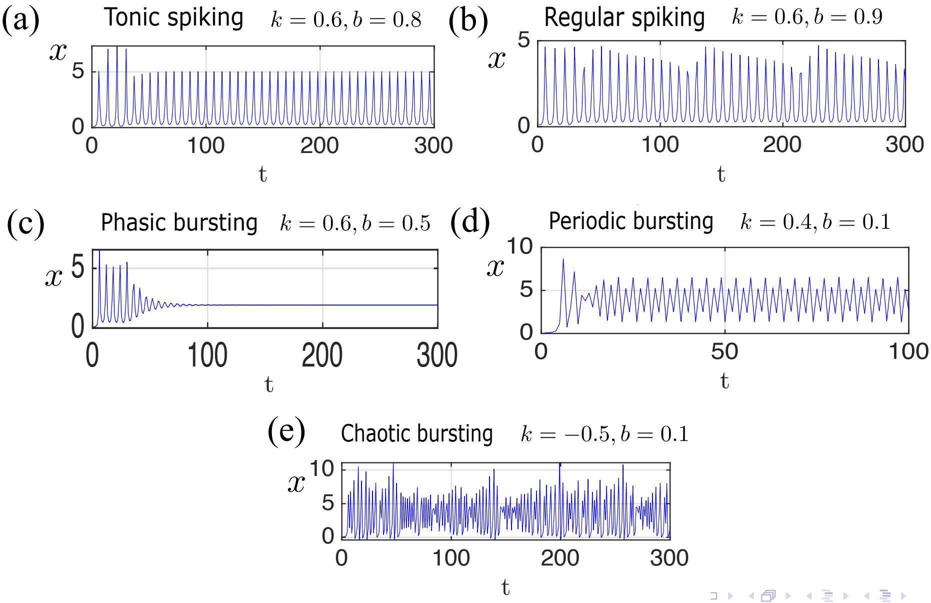

Ring-star network for multiple neurons

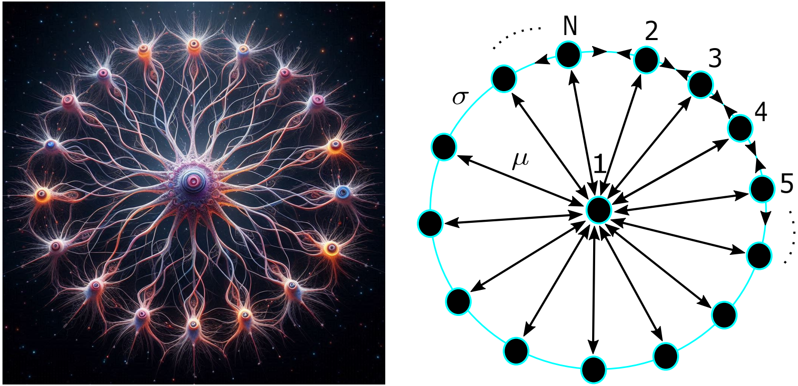

(a) (b)

Figure: (a) Ensemble of connected neurons. (Powered by DALL-E 3). (b) Ring-star network of Chialvo neuron system.

Ring-star network for multiple neurons

- The mathematical model for the ring-star connected Chialvo neuron map under electromagnetic flux is defined as:

$$
\begin{aligned}
x_m(n+1) &= x_m(n)^2 e^{y_m(n)-x_m(n)} + k_0 + k x_m(n) M(\phi_m(n)) \\
&\quad + \mu(x_m(n) - x_1(n)) + \frac{\sigma}{2R} \sum_{i=m-R}^{m+R} (x_i(n) - x_m(n)), \\
y_m(n+1) &= a y_m(n) - b x_m(n) + c, \\
\phi_m(n+1) &= k_1 x_m(n) - k_2 \phi_m(n),
\end{aligned}
$$

Ring-star network for multiple neurons

- The central node is further defined as

$$
\begin{aligned}
x_1(n+1) &= x_1(n)^2 e^{(y_1(n)-x_1(n))} + k_0 + k x_1(n) M(\phi_1(n)) \\
&+ \mu \sum_{i=1}^{N} (x_i(n) - x_1(n)), \\
y_1(n+1) &= a y_1(n) - b x_1(n) + c, \\
\phi_1(n+1) &= k_1 x_1(n) - k_2 \phi_1(n),
\end{aligned}
$$

having the following boundary conditions:

$$
\begin{aligned}
x_{m+N}(n) &= x_m(n), \\
y_{m+N}(n) &= y_m(n), \\
\phi_{m+N}(n) &= \phi_m(n).
\end{aligned} \tag{1}
$$

Simulations

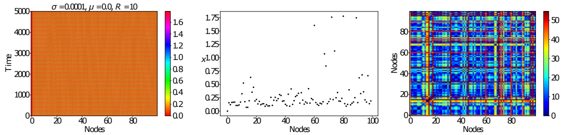

(a) Unsynchronized state

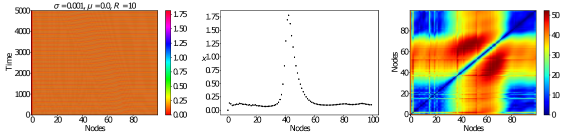

(b) Chimera state

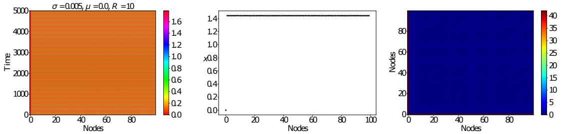

(c) Synchronized state

Simulations

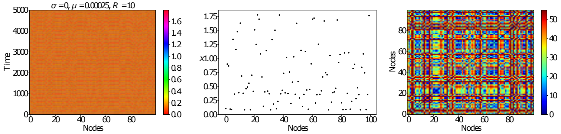

(a) Unsynchronized state

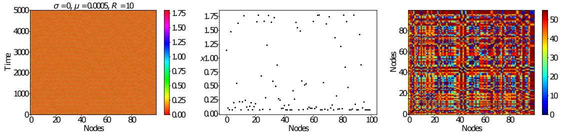

(b) Transition to two-clustered state

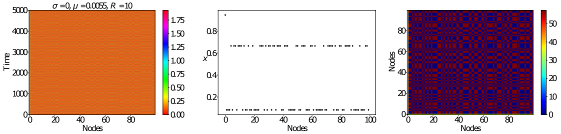

(c) Two-clustered state

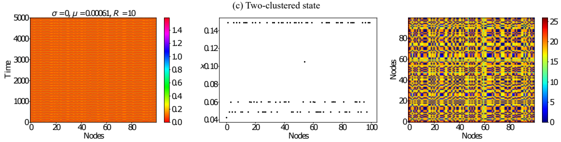

(d) Three-clustered state

Heterogeneous coupling strengths (Ghosh, Muni, & Fatoyinbo, 2023)

Nonlinear Dyn (2023) 111:17499–17518
https://doi.org/10.1007/s11071-023-08717-y

ORIGINAL PAPER

On the analysis of a heterogeneous coupled network of memristive Chialvo neurons

Indranil Ghosh · Sishu Shankar Muni · Hammed Olawale Fatoyinbo

Heterogeneous coupling strengths (Ghosh, Muni, & Fatoyinbo, 2023)

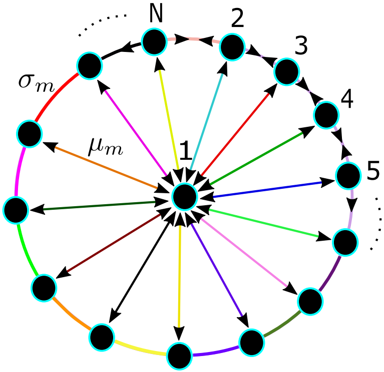

Figure: The star and ring coupling strengths are denoted by μ_m and σ_m for each node $m = 1, \dots, N$ respectively. Different colors in the ring-star topology signify a range of heterogeneous values of μ_m and σ_m.

Heterogeneous coupling strengths (Ghosh, Muni, & Fatoyinbo, 2023)

- We introduce heterogeneities to the coupling strengths $\sigma_m(n)$ and $\mu_m(n)$ both in space and time.
- In space, the heterogeneities are realized following the application of a noise source with a uniform distribution given by

$$\sigma_m(n) = \sigma_0 + D_\sigma \xi_\sigma^{m,n}, \tag{2}$$
$$\mu_m(n) = \mu_0 + D_\mu \xi_\mu^{m,n}, \tag{3}$$

- Here σ_0 and μ_0 are the mean values of the coupling strengths μ_m and σ_m respectively.
- We keep $\sigma_0 \in [-0.01, 0.01]$ and $\mu_0 \in [-0.001, 0.001]$.
- The noise sources ξ_σ and ξ_μ for the corresponding coupling strengths are real numbers randomly sampled from the uniform distribution $[-0.001, 0.001]$.
- Finally, the D's refer to the "noise intensity" which we restrict in the range $[0, 0.1]$.

Heterogeneous coupling strengths (Ghosh, Muni, & Fatoyinbo, 2023)

- Heterogeneity in time is introduced by considering the network having time-varying links depending on the two coupling probabilities P_μ and P_σ, which govern the update of the coupling topology with each iteration n.
- The probability with which the central node is connected to all the peripheral nodes at a particular n is denoted by P_μ.
- Likewise, the probability with which the peripheral nodes are connected to their R neighboring nodes is given by P_σ.
- We employ three metrics to analyse our model: (1) *cross-correlation coefficient*, (2) *synchronization error*, and (3) Sample entropy

Quantitative metrics

- The general definition of the cross-coefficient denoted by $\Gamma_{\mathrm{i,m}}$ is given by

$$\Gamma_{\mathrm{i,m}} = \frac{\langle \tilde{x}_i(n)\tilde{x}_m(n)\rangle}{\sqrt{\langle(\tilde{x}_i(n))^2\rangle\langle(\tilde{x}_m(n))^2\rangle}}. \tag{4}$$

- The *averaged cross-correlation coefficient* over all the units of the network is given by,

$$\Gamma = \frac{1}{N-1}\sum_{m=1,m\neq i}^{N}\Gamma_{\mathrm{i,m}}. \tag{5}$$

- We use $\Gamma_{2,m}$, denoting the degree of correlation between the first peripheral node of the ring-star network and all the other nodes, including the central node.
- The average is calculated over time with transient dynamics removed and $\tilde{x}(n) = x(n) - \langle x(n)\rangle$.

Quantitative metrics

- The averaged *synchronization-error* for the nodes in a system is given by

$$E = \frac{1}{N-1} \sum_{m=1, m \neq 2}^{N} \langle |x_2(n) - x_m(n)| \rangle, \tag{6}$$

- We again consider node number $N = 2$ as the baseline.

Simulations

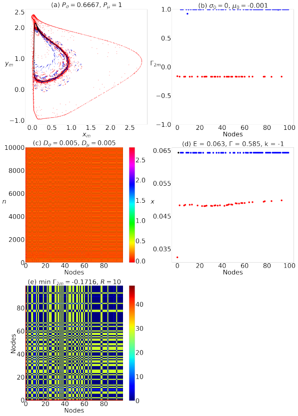

Figure: Coherent and solitary nodes giving rise to a two-clustered state.

simulations

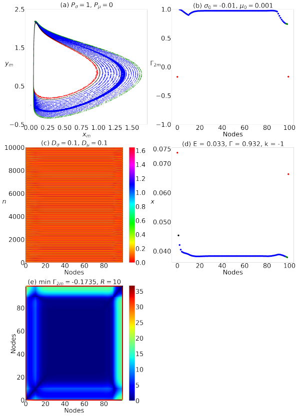

Figure: Mostly synced in the coherent domain with two solitary nodes.

Simulations

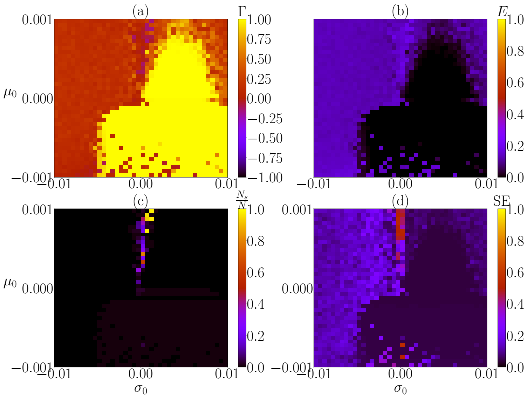

Figure: An almost definitive bifurcation boundary is observed. Solitary nodes appear around $\sigma_0 \sim 0$ and $\mu_0 > 0$.

Simulations

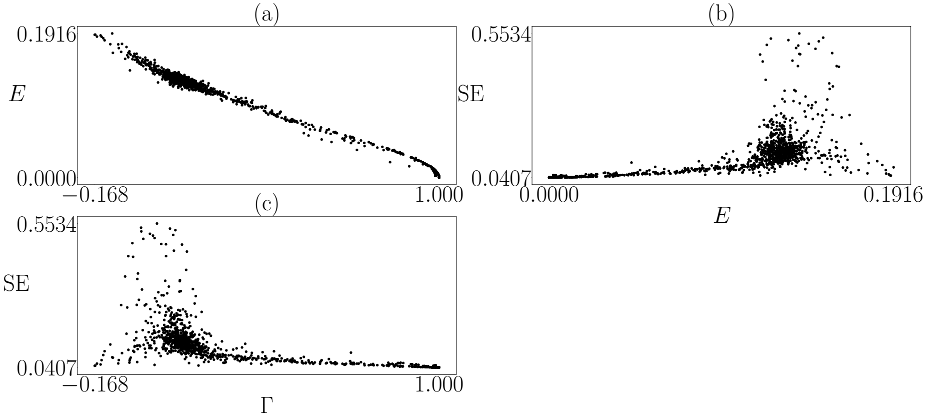

Figure: Comparison plots for the various measures. Figures (a) and (c) show an inverse trend whereas figure (b) shows a proportional trend.

A bit of a digression! (Ghosh, Nair, Fatoyinbo, & Muni, 2024)

Eur. Phys. J. Plus (2024) 139:545
https://doi.org/10.1140/epjp/s13360-024-05363-0

THE EUROPEAN PHYSICAL JOURNAL PLUS

Regular Article

Check for updates

Dynamical properties of a small heterogeneous chain network of neurons in discrete time

Indranil Ghosh[1,a], **Anjana S. Nair**[2,b], **Hammed Olawale Fatoyinbo**[3,4,c], **Sishu Shankar Muni**[2,d]

[1] School of Mathematical and Computational Sciences, Massey University, Colombo Road, Palmerston North 4410, New Zealand
[2] School of Digital Sciences, Digital University Kerala, Technopark Phase-IV Campus, Mangalapuram, Kerala 695317, India
[3] EpiCentre, School of Veterinary Science, Massey University, Palmerston North 4410, New Zealand
[4] Department of Mathematical Sciences, Auckland University of Technology, Auckland 1010, New Zealand

Received: 25 March 2024 / Accepted: 13 June 2024

A bit of a digression! (Ghosh, Nair, Fatoyinbo, & Muni, 2024)

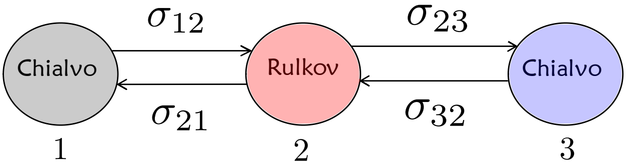

Figure: A heterogeneous network of a tri-oscillator chain composed of end nodes (Chialvo neuron map) and central node (Rulkov neuron map).

Higher-order smallest ring-star network (Nair, Ghosh, Fatoyinbo, & Muni, 2024)

On the higher-order smallest ring-star network of Chialvo neurons under diffusive couplings

Cite as: Chaos **34**, 073135 (2024); doi: 10.1063/5.0217017
Submitted: 2 May 2024 · Accepted: 3 July 2024 ·
Published Online: 18 July 2024

View Online Export Citation CrossMark

Anjana S. Nair,[1] Indranil Ghosh,[2,a)] Hammed O. Fatoyinbo,[3] and Sishu S. Muni[1]

AFFILIATIONS

[1] School of Digital Sciences, Digital University Kerala, Technopark Phase-IV campus, Mangalapuram 695317, Kerala, India
[2] School of Mathematical and Computational Sciences, Massey University, Colombo Road, Palmerston North 4410, New Zealand
[3] Department of Mathematical Sciences, School of Engineering, Computer and Mathematical Sciences, Auckland University of Technology, Auckland 1142, New Zealand

[a)] **Author to whom correspondence should be addressed:** i.ghosh@massey.ac.nz

Higher-order smallest ring-star network (Nair, Ghosh, Fatoyinbo, & Muni, 2024)

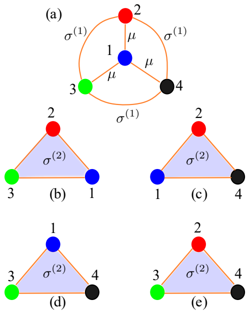

Figure: In panel (a) the coupling strength within the star configuration is denoted by μ, while the coupling strength within the ring is denoted by $\sigma^{(1)}$. Moreover, the coupling strength originated from the higher-order interactions is represented by $\sigma^{(2)}$, as indicated by the triplets in panels (b)$\rightarrow$(e).

Model

This system in compact form is written as

$$
\begin{aligned}
x_p(n+1) &= x_p(n)^2 e^{(y_p(n)-x_p(n))} + k_0 + \mu(x_1(n) - x_p(n)) \\
&\quad + \sigma^{(1)} \sum_{i=2}^{4} (x_i(n) - x_p(n)) \\
&\quad + \sigma^{(2)} \sum_{i=1}^{4} \sum_{\substack{j=i+1 \\ i \neq p \\ j \neq p}}^{4} (x_i(n) + x_j(n) - 2x_p(n)), \qquad (7) \\
y_p(n+1) &= a y_p(n) - b x_p(n) + c, \qquad (8)
\end{aligned}
$$

Model

and

$$x_1(n+1) = x_1(n)^2 e^{(y_1(n) - x_1(n))} + k_0 + \mu \sum_{i=2}^{4} (x_i(n) - x_1(n))$$
$$+ \sigma^{(2)} \sum_{i=2}^{4} \sum_{j=i+1}^{4} (x_i(n) + x_j(n) - 2x_1(n)), \tag{9}$$
$$y_1(n+1) = ay_1(n) - bx_1(n) + c. \tag{10}$$

Simulations

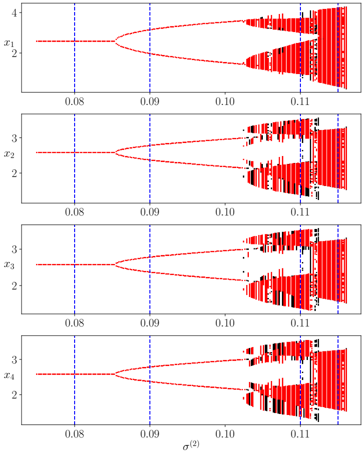

Figure: Bifurcation plot of each node against the coupling strength $\sigma^{(2)}$ once simulated forward (points colored black) and once backward (points colored red).

Simulations

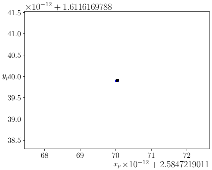

(a) $\sigma^{(2)} = 0.08$

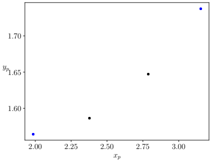

(b) $\sigma^{(2)} = 0.09$

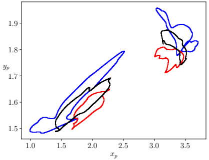

(c) $\sigma^{(2)} = 0.11$

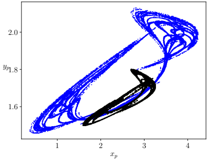

(d) $\sigma^{(2)} = 0.115$

Figure: Typical phase portraits. (a) fixed point, (b) period-doubling, (c) a disjoint cyclic quasiperiodic closed invariant curve, (d) chaos.

$0 - 1$ test

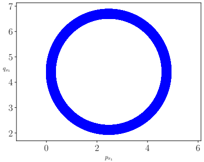

(a) $\sigma^{(2)} = 0.08$

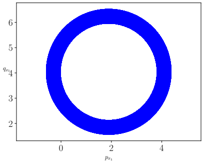

(b) $\sigma^{(2)} = 0.09$

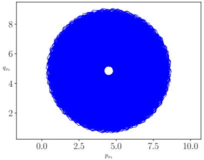

(c) $\sigma^{(2)} = 0.11$

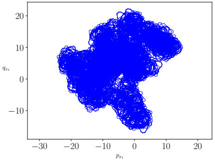

(d) $\sigma^{(2)} = 0.115$

Figure: Signal plots. (a) highly bounded trajectory, (b) slightly less bounded trajectory, (c) between bounded and diffusive, and (d) diffusive random walk corresponding to a Brownian motion with zero drift.

Metrics

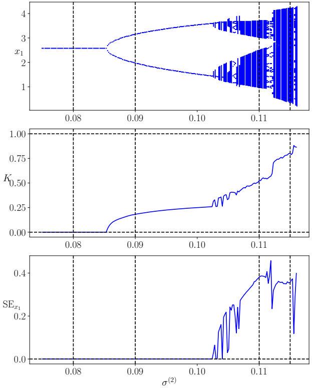

Figure: A bifurcation plot of the first node with $\sigma^{(2)}$ as the main bifurcation parameter. The corresponding value of K from the chaos test and SE for complexity are shown.

Denatured Morris-Lecar model (Fatoyinbo *et al.*, 2022)

2022 International Conference on Decision Aid Sciences and Applications (DASA)

Numerical Bifurcation Analysis of Improved Denatured Morris-Lecar Neuron Model

Hammed Olawale Fatoyinbo
School of Mathematical and Computational Sciences
Massey University
Palmerston North, New Zealand
h.fatoyinbo@massey.ac.nz
ORCID: 0000-0002-6036-2957

Sishu Shankar Muni
School of Mathematical and Computational Sciences
Massey University
Palmerston North, New Zealand
s.muni@massey.ac.nz
ORCID: 0000-0001-9545-8345

Indranil Ghosh
School of Mathematical and Computational Sciences
Massey University
Palmerston North, New Zealand
i.ghosh@massey.ac.nz

Ibrahim Olatunji Sarumi
Department of Mathematics and Statistics
King Fahd University of Petroleum and Minerals
Dhahran, Saudi Arabia
isarumi@kfupm.edu.sa

Afeez Abidemi
Department of Mathematical Sciences
Federal University of Technology
Akure, Nigeria
aabidemi@futa.edu.ng
ORCID: 0000-0003-1960-0658

Denatured Morris-Lecar model (Fatoyinbo *et al.*, 2022)

The dentaured Morris-Lecar model proposed in the book[1]consists of two nonlinearly coupled ODEs

$$\dot{x} = x^2(1 - x) - y + I, \tag{11}$$

$$\dot{y} = Ae^{\alpha x} - \gamma y. \tag{12}$$

Here x is the action potential, y is again the recovery variable and I is the external current. The other parameters are all positive constants.

[1]D. Schaeffer and J. Cain, *Ordinary differential equations: Basics and beyond* (Springer, 2018)

New Model

$$\dot{x} = x^2(1-x) - y + I, \tag{13}$$
$$\dot{y} = Ae^{\alpha x} - \gamma y, \tag{14}$$
$$\dot{I} = \varepsilon(I'(x) - I), \tag{15}$$

where

$$I'(x) = \frac{1}{60}\left[1 + \tanh\left(\frac{0.05 - x}{0.001}\right)\right] \tag{16}$$

is the smoothed-out version of the step function given by

$$H(x) = \begin{cases} \frac{1}{30}, & x < 0.05, \\ 0, & x > 0.05. \end{cases} \tag{17}$$

New Model

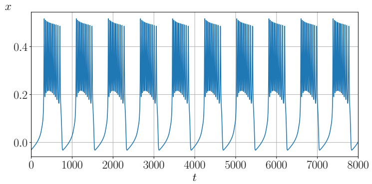

(a) Time series

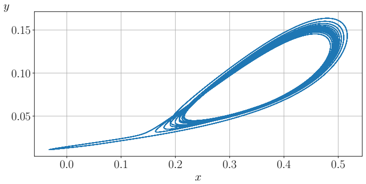

(b) Phase portrait

The End

Thank you! Questions?